

# COMPARISON OF RF CAVITY TRANSPORT MODELS FOR BBU SIMULATIONS\*

I. Shin<sup>1</sup>, B. Yunn<sup>2</sup>, T. Satogata<sup>2</sup>, S. Ahmed<sup>2</sup>

<sup>1</sup>Department of Physics, University of Connecticut, CT 06269, USA

<sup>2</sup>Thomas Jefferson National Accelerator Facility, Newport News, VA 23606, USA

## Abstract

The transverse focusing effect in RF cavities plays a considerable role in beam dynamics for low-energy beamline sections and can contribute to beam breakup (BBU) instability. The purpose of this analysis is to examine RF cavity models in simulation codes which will be used for BBU experiments at Jefferson Lab and improve BBU simulation results. We review two RF cavity models in the simulation codes *elegant* and *TDBBU* (a BBU simulation code developed at Jefferson Lab). *elegant* can include the Rosenzweig-Serafini (R-S) model for the RF focusing effect. Whereas *TDBBU* uses a model from the code *TRANSPORT* which considers the adiabatic damping effect, but not the RF focusing effect. Quantitative comparisons are discussed for the CEBAF beamline. We also compare the R-S model with the results from numerical simulations for a CEBAF-type 5-cell superconducting cavity to validate the use of the R-S model as an improved low-energy RF cavity transport model in *TDBBU*. We have implemented the R-S model in *TDBBU*. It will cause BBU simulation results to be better matched with analytic calculations and experimental results.

## INTRODUCTION

In recirculating accelerators such as CEBAF at Jefferson Lab, the multipass BBU phenomena can limit the maximum current, which depends on recirculating beamline optics as well as RF cavity properties. The recirculating beamline optics can be affected by the RF focusing in a low-energy beamline section. For BBU experiments at Jefferson Lab we discuss the RF cavity models, which can affect beamline optics and the BBU threshold current.

*elegant* [1] calculates beamline optics and *TDBBU* [2] computes BBU threshold currents using optics calculation results from *elegant*. The *elegant* optics calculations are also used for beamline setups for the BBU experiments, and to provide transfer matrices for theoretical calculations of BBU threshold currents. The two simulation codes should treat beamline elements in the same manner for agreement between simulations and experiments, but they do not. The nominal CEBAF beamline optics for *elegant* employ the RF focusing effect using the R-S model [3]. On the other hand *TDBBU* does not have the RF focusing feature, which is important in understanding beam dynamics in low energy sections such as electron guns and low

energy portions of linacs.

For the comparison of the two models, we review the generic transfer matrices of a simple acceleration model and the R-S model. Beta functions and transfer matrices for the CEBAF beamlines are illustrated for the two models. The R-S model is compared to the numerical calculations by Zenghai Li using *MAFIA* and *PARMELA* for a CEBAF-type 5-cell superconducting cavity [4]. This comparison justifies the use of R-S model for CEBAF-type cavities to incorporate the RF focusing effect.

## COMPARISON OF RF CAVITY TRANSPORT MODELS

The transfer matrix elements in the following section refer to the elements in the form of:

$$\begin{pmatrix} x \\ x' \end{pmatrix} = \begin{pmatrix} M_{11} & M_{12} \\ M_{21} & M_{22} \end{pmatrix} \begin{pmatrix} x_0 \\ x'_0 \end{pmatrix}. \quad (1)$$

### Cavity Model in *TDBBU*

*TDBBU* has the same accelerating cavity model as the model in *TRANSPORT* [5]. This model does not include any focusing effects. It treats an RF cavity as a simple accelerating section with constant energy gain throughout the RF cavity. For ultra-relativistic particles ( $\beta c \cong c$ ), the transfer matrix elements in *TDBBU* are:

$$\begin{cases} M_{11} = 1 \\ M_{12} = L \frac{\gamma_i}{\Delta\gamma \cos(\Delta\phi)} \ln \left( 1 + \frac{\Delta\gamma \cos(\Delta\phi)}{\gamma_i} \right) \\ M_{21} = 0 \\ M_{22} = \frac{\gamma_i}{\gamma_i + \Delta\gamma \cos(\Delta\phi)}, \end{cases} \quad (2)$$

where  $L$  is the length of the cavity,  $\gamma_i$  is the Lorentz factor at the entrance of the cavity,  $\Delta\gamma$  is the difference in Lorentz factors between the entrance and exit of the cavity, and  $\Delta\phi$  is the phase of the particle with respect to the maximum acceleration phase.

### R-S Model

In a cylindrically symmetric and spatially periodic RF cavity, the accelerating RF field,  $E_z$ , induces fields in the radial and azimuthal directions. These induced fields generate a force in the radial direction, given by  $F_r \cong -\frac{qr}{2} \frac{d}{dz} E_z$  [6] [7], where  $q$  is the charge of the particle. The R-S model combines the focusing effects by this radial force and end-focusing effects due to the fringe fields at the entrance and exit of the cavity. These effects can be

\* Work supported by DOE contract DE-AC05-06OR23177.

incorporated into a single transfer matrix for an RF cavity of arbitrary modes [3]. For a pure  $\pi$  mode cavity, this model simplifies to the Chambers model [8] and the transfer matrix reduces to [3]:

$$\begin{cases} M_{11} = \cos \alpha - \sqrt{2} \cos(\Delta\phi) \sin \alpha \\ M_{12} = \sqrt{8} \frac{\gamma_f}{\gamma_i} \cos(\Delta\phi) \sin \alpha \\ M_{21} = -\frac{\gamma_f}{\gamma_i} \left( \frac{\cos(\Delta\phi)}{\sqrt{2}} + \frac{1}{\sqrt{8} \cos(\Delta\phi)} \right) \sin \alpha \\ M_{22} = \frac{\gamma_i}{\gamma_f} (\cos \alpha + \sqrt{2} \cos(\Delta\phi) \sin \alpha), \end{cases} \quad (3)$$

where  $\gamma_f$  is the Lorentz factor at the exit of the cavity,  $\gamma_i$  is the normalized energy gradient averaged over the RF structure, and  $\alpha \equiv \frac{1}{\sqrt{8} \cos(\Delta\phi)} \ln \left( \frac{\gamma_f}{\gamma_i} \right)$ .

### Comparison of Two Models for CEBAF Beam-lines

Figure 1 shows the beta functions of the north linac for the nominal beamline setup using the R-S model. Electrons with 45 MeV are injected into the north linac and acquire 400 MeV energy gain. When the RF focusing effect is not included in the north linac optics, the beta functions show quite different behavior because of mismatching as shown in Figure 2.

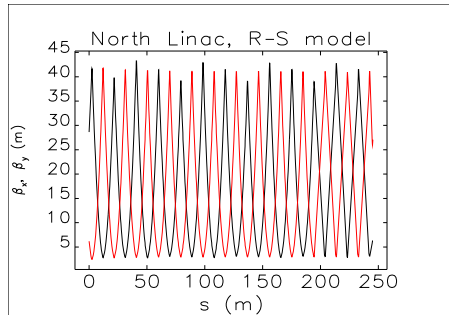


Figure 1: Beta functions for the north linac when the R-S model is applied. The black line (solid) is  $\beta_x$  and the red one (dotted)  $\beta_y$ .

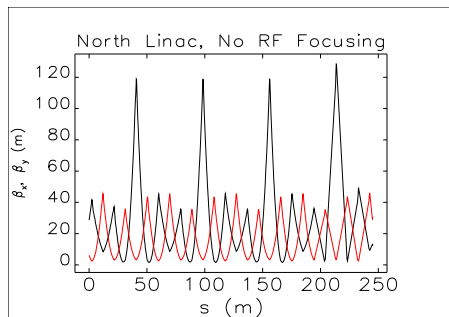


Figure 2: Beta functions for the north linac without the RF focusing effect.

When the R-S model is applied to the north linac, the full transfer matrix for the north linac in  $(x, x', y, y')$  phase

### Beam Dynamics and EM Fields

#### Dynamics 01: Beam Optics (lattices, correction, transport)

space is

$$\begin{pmatrix} -3.89 \times 10^{-1} & 3.94 & 0 & 0 \\ -9.42 \times 10^{-4} & -2.50 \times 10^{-1} & 0 & 0 \\ 0 & 0 & 3.67 \times 10^{-1} & 3.45 \\ 0 & 0 & -1.29 \times 10^{-2} & 1.54 \times 10^{-1} \end{pmatrix},$$

and the transfer matrix of the linac without the focusing effects is

$$\begin{pmatrix} -2.61 \times 10^{-1} & 4.63 & 0 & 0 \\ -1.17 \times 10^{-2} & -1.79 \times 10^{-1} & 0 & 0 \\ 0 & 0 & 6.07 \times 10^{-1} & 4.09 \\ 0 & 0 & 1.11 \times 10^{-2} & 2.42 \times 10^{-1} \end{pmatrix}.$$

The differences in the beta functions and the matrix elements for the north linac are considerable, whereas the south linac does not show a difference as much as in the north linac as shown in Figure 3 and 4. This is because the beam energy in the south linac is higher than in the north linac so that the RF focusing effect becomes much weaker. Electrons with 450 MeV go into the south linac through which electrons obtain 400 MeV.

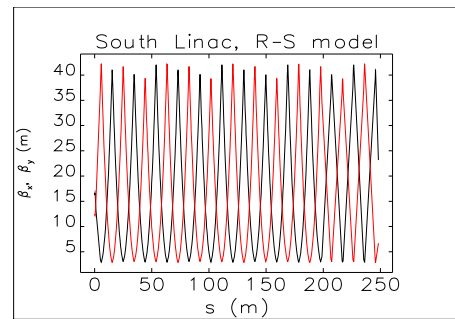


Figure 3: Beta functions for the south linac when the R-S model is applied.

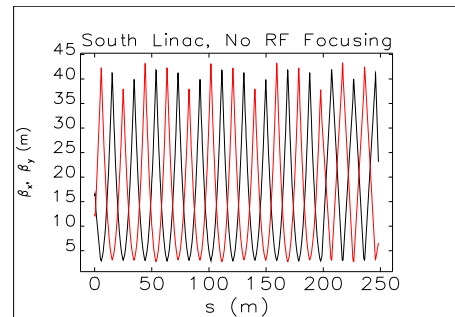


Figure 4: Beta functions for the south linac without the RF focusing effect.

The transfer matrix for the south linac with the RF focusing effect is

$$\begin{pmatrix} -9.48 \times 10^{-1} & 1.23 \times 10^1 & 0 & 0 \\ 1.07 \times 10^{-1} & -1.94 & 0 & 0 \\ 0 & 0 & -1.11 \times 10^{-2} & 6.11 \\ 0 & 0 & -8.76 \times 10^{-2} & 7.64 \times 10^{-1} \end{pmatrix}$$

and the transfer matrix of the linac without the RF focusing effect is

$$\begin{pmatrix} -9.33 \times 10^{-1} & 1.25 \times 10^1 & 0 & 0 \\ 1.06 \times 10^{-1} & -1.97 & 0 & 0 \\ 0 & 0 & 6.26 \times 10^{-2} & 6.33 \\ 0 & 0 & -7.50 \times 10^{-2} & 8.21 \times 10^{-1} \end{pmatrix}$$

These differences in beta functions and the matrix elements influence on the simulations for the BBU threshold currents. Beamline setups for the BBU experiments will be accomplished based on optics calculations from *elegant* and the transfer matrices for analytic calculations will also be obtained from *elegant*. Therefore *TDBBU* should include the RF focusing effect in the same manner as in *elegant* to simulate BBU phenomena and compare the results to the analytic calculations and experimental results.

### Comparison of R-S Model with Numerical Simulation Results

As part of a beam dynamics study in a CEBAF 5-cell superconducting cavities by Zenghai Li, the transverse focusing effect was studied by numerical methods using *MAFIA* and *PARMELA* [4]. Focal lengths obtained from the numerical methods and the R-S model are listed in Table 1. The focal length computed from the numerical methods is proportional to  $\gamma^2$  as predicted theoretically by G. A. Krafft [9].

Table 1: Beam energy and focal lengths calculated from the R-S model and the numerical simulations.  $E_k$  stands for kinetic energy,  $\gamma$  is the Lorentz factor,  $f_{RS}$  is the focal length obtained from the R-S model, and  $f_{map}$  is the focal length obtained from the numerical methods [10].

$E_k [MeV]$	$\gamma$	$f_{RS} [m]$	$f_{map} [m]$
0.5	1.98	0.12	4.46
2.5	5.89	1.79	4.50
5.0	10.79	6.33	10.71
10.0	20.57	23.41	31.17
20.0	40.14	89.59	107.00
40.0	79.28	349.95	390.98
100.0	196.69	2155.03	2213.82

The ratio of the two focal lengths in Table 1 are plotted with respect to beam energy in Figure 5. The R-S model assumes ultra-relativistic particles so that the two results do not agree with each other in very low energy, but the two focal lengths become closer as a particle energy increases. There exists about 10% difference between the two methods around 45 MeV, which is an injection energy to the north linac. Figure 5 shows the R-S model is a good approximation for higher energy than the injection energy of 45 MeV.

### CONCLUSIONS

The RF focusing effect gives recognizable influence on the beam dynamics for the first pass in CEBAF machine. In order to incorporate this effect into BBU simulations, we have implemented the RF focusing feature in *TDBBU* using the R-S model. It will cause BBU simulations to be better matched with analytic calculations and experimental results.

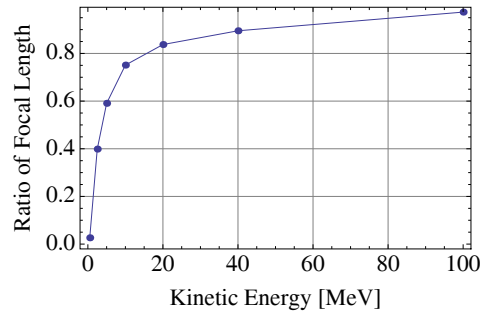


Figure 5: Ratio of focal lengths versus kinetic energy. The vertical axis is the focal length ratio of the R-S model to the numerical methods.

### ACKNOWLEDGMENTS

The authors are indebted to Z. Li for his Ph.D. dissertation which provided us valuable data to work with. An author, I. Shin, would like to thank his advisor, K. Joo, for supporting him.

### REFERENCES

- [1] M. Borland, “elegant: A Flexible SDDS-Compliant Code for Accelerator Simulation”, Advanced Photon Source LS-287, September 2000.
- [2] G. A. Krafft, J. J. Bisognano, “Two Dimensional Simulations of Multipass Beam Breakup”, PAC 1987, pg. 1356 (1987).
- [3] J. Rosenzweig, L. Serafini, “Transverse Particle Motion in Radio-frequency Linear Accelerators”, Phys. Rev. E **49**, 2 (1994).
- [4] Z. Li, Ph.D. thesis, “Beam Dynamics in the CEBAF Superconducting Cavities”, College of William & Mary, Williamsburg, VA (1995).
- [5] D. Carey, K. Brown, F. Rothacker, “Third-order TRANSPORT, a Computer Program for Designing Charged Particle Beam Transport Systems”, SLAC-R-95-462, Fermilab-Pub-95/069, UC-414, P. 180 (1995).
- [6] R. H. Helm and R. Miller, in *Linear Accelerators*, ed. P. M. Lapostolle and A. L. Septier, North-Holland, Amsterdam, pg. 115 (1970).
- [7] S. Hartman, J. Rosenzweig, “Ponderomotive Focusing in Axisymmetric RF Linacs”, Phys. Rev. E **47**, 3 (1993).
- [8] P. Piot, G. A. Krafft, “Transverse RF Focussing in Jefferson Lab Superconducting Cavities”, EPAC 1998, pg. 1327 (1998).
- [9] G. A. Krafft, “More on the Transfer Matrix of a Cavity”, JLAB Technical Report No. CEBAF-TN-91-069, 1991.
- [10] The  $f_{map}$  data for 20 and 40 MeV were obtained from the data points on Figure 3-16 in the dissertation of Zenghai Li.